Properties of the cAMP-activated Cl^- current in choroid plexus epithelial cells isolated from the rat

Jonathan D. Kibble, Ann E. O. Trezise* and Peter D. Brown

*Cell Physiology Group, School of Biological Sciences, University of Manchester, G.38, Stopford Building, Oxford Road, Manchester M13 9PT and *Nuffield Department of Clinical Biochemistry, University of Oxford, John Radcliffe Hospital, Oxford OX3 9DU, UK*

1. This study used whole-cell patch clamp and RNA *in situ* hybridization experiments to determine whether the cAMP-activated Cl^- current expressed in choroid plexus epithelial cells was carried by the cystic fibrosis transmembrane conductance regulator (CFTR) channel.

2. In patch clamp experiments, inclusion of 0·25 mM cAMP and 375 nM protein kinase A catalytic subunit (PKA) in the electrode solution caused activation of an inwardly rectifying current (21/23 cells). This current was Cl^- selective, since the current reversal potential (E_{rev}) was -31 ± 3 mV with equilibrium potential values for Cl^- (E_{Cl}) and Na^+ (E_{Na}) of -44 and 0 mV, respectively.

3. In anion substitution experiments, the relative anion permeability sequence for the inward rectifier was: I^- (3·5) > HCO_3^- (1·5) = Cl^- (1·0) > Br^- (0·6) > aspartate (0·2).

4. The inward rectifier was sensitive to inhibition by a range of known channel inhibitors, including: glibenclamide (100 μM), DIDS (100 and 500 μM), NPPB (100 μM) and Ba^{2+} (1 mM).

5. In RNA *in situ* hybridization experiments, using two independent rat CFTR cRNA probes, expression of CFTR could not be detected in epithelial cells from the rat choroid plexus.

6. In conclusion, the cAMP-dependent whole-cell Cl^- current present in choroid plexus epithelial cells from the rat has properties which are distinctly different from those of CFTR.

The choroid plexuses are epithelial tissues which project into the ventricles of the brain, and are responsible for secreting cerebrospinal fluid (CSF) (Segal, 1993). Regulation of CSF production is thought to involve anion channels located in the apical (ventricle-facing) plasma membrane, one or more of which are activated by cAMP (Saito & Wright, 1983; Deng & Johanson, 1992). These channels mediate the efflux of Cl^- and HCO_3^- from the cell, which in turn drives Na^+ and water fluxes resulting in increased CSF production. This process of secretion is similar to that described in several other epithelia, notably those at sites such as the airways, gut, pancreas and sweat glands in which the cystic fibrosis transmembrane conductance regulator (CFTR) Cl^- channel is expressed (Fuller & Benos, 1992). Failure to express CFTR in these epithelia results in reduced fluid secretion and leads to complications associated with the disease cystic fibrosis.

It was reported recently that CFTR is expressed in epithelial cells of the rat choroid plexus (Hincke, Nairn & Staines, 1995). This observation is somewhat unexpected, since there is no evidence that the choroid plexus is affected in cystic fibrosis. However, the possibility remains that CFTR, if present, could contribute to cAMP-activated anion currents in the choroid plexus. A cAMP-activated Cl^- current with an inwardly rectifying current–voltage (I–V) relationship was recently identified in the rat choroid plexus (Kotera & Brown, 1994*a*). This differs from the characteristic linear current generally associated with CFTR (Kartner *et al.* 1991), suggesting that the predominant cAMP-dependent Cl^- current in the choroid plexus may be distinct from that of CFTR.

The aim of the present study was to characterize the inwardly rectifying Cl^- current in the rat choroid plexus and to compare its properties with current associated with other known Cl^- channels, particularly CFTR. In addition, the expression of CFTR in rat choroid plexus was assessed using the specific and sensitive method of RNA *in situ* hybridization.

METHODS

Patch clamp recording

Adult male Sprague–Dawley rats (Charles River, Kent, UK) were killed by an overdose of chloroform and the choroid plexus was dissected from the fourth ventricle. The tissue was placed in control bath solution (see below) and was used within 3 h. The conventional whole-cell recording method (Hamill, Marty, Neher, Sakmann & Sigworth, 1981) was applied to measure membrane currents in cells of isolated, intact choroid plexus. The intact tissue may be used for patch clamping because little cell-to-cell coupling exists between epithelial cells of the choroid plexus (Saito & Wright, 1984; Kotera & Brown, 1994*b*). A small piece of tissue (2–3 mm) was secured with a stainless steel wire to the base of a perfusion chamber (bath volume, 0·4 ml), which was mounted on the stage of an inverted microscope (Olympus IMT-2, Japan). Gigaohm seals could be obtained on the exposed apical (ventricular) membrane of the epithelial cells.

Patch pipettes were made from haematocrit capillary tubes (Oxford Labware, St Louis, MO, USA) using a two-stage vertical puller (PB-7; Narishige, Japan). The tip resistances of the patch electrodes were 3–5 MΩ. Membrane currents were measured using an Axopatch-1D amplifier (Axon Instruments, Foster City, CA, USA). Step voltage pulses were generated by computer using pCLAMP software (version 5.5.1; Axon Instruments) and a TL-1 interface (Axon). Data were stored on the computer hard disk. In all experiments cell capacitance was maximally compensated. The series resistance was not compensated in this study. All experiments were carried out at room temperature (19–23 °C). Bath and pipette electrodes were connected to ground via Ag–AgCl pellets.

The control pipette solution contained (mM): 20 NaCl, 110 sodium aspartate, 3 $MgCl_2$, 5 Na_2ATP, 5 BAPTA (Sigma), 10 Hepes, 10 glucose; pH 7·2; osmolality, 297 mosmol kg^{-1}. The control bath solution contained (mM): 140 NaCl, 1 $MgCl_2$, 1 $CaCl_2$, 10 Hepes, 10 glucose, 15 mannitol; pH 7·3; osmolality, 299 mosmol kg^{-1}. Activation of the inward rectifier was achieved by including 0·25 mM cAMP (Sigma) and 375 nM protein kinase A catalytic subunit (PKA; Promega, Southampton, UK) in the electrode solution. In experiments to investigate the importance of cell swelling, the control electrode solution was made hypertonic (osmolality, 328 mosmol kg^{-1}) by addition of 30 mM mannitol.

To determine relative anion selectivity properties of the inward rectifier, separate groups of experiments were performed in which currents were activated in the presence of different intracellular halides. Pipette solutions contained: 110 mM NaX^-, 12 mM NaCl, 3 mM $MgCl_2$, 5 mM Na_2ATP, 5 mM BAPTA, 10 mM Hepes, 10 mM glucose, 0·25 mM cAMP and 375 nM PKA; pH, 7·2; where X^- represents a replacement halide (either iodide or bromide). The corresponding bath solutions contained (mM): 110 NaCl, 12 NaX^-, 1 $CaCl_2$, 1 $MgCl_2$, 10 Hepes, 10 glucose, 40 mannitol; pH 7·3. Using these conditions, the equilibrium potentials E_{Cl} (−47 mV) and E_X (+56 mV) were well separated so that, in addition to differences in whole-cell conductance, the sign and magnitude of current reversal potentials (E_{rev}) could be used to indicate the relative anion permeability (P_X/P_{Cl}). Since P_{Cl} is known to exceed P_{Na} by a factor of approximately 50 (Kotera & Brown, 1994*a*), we have made the assumption that Cl^- and X^- were the only permeant ions and applied the Goldman–Hodgkin–Katz voltage equation to calculate P_X/P_{Cl}:

$$E_{rev} = \left(\frac{RT}{F}\right)\ln\left(\frac{([Cl^-]_i + (P_X/P_{Cl})[X^-]_i)}{([Cl^-]_o + (P_X/P_{Cl})[X^-]_o)}\right), \quad (1)$$

where E_{rev} is the reversal potential, $[Cl^-]$ and $[X^-]$ are the concentrations of Cl^- and replacement anion X^-, and subscripts i and o denote intracellular and extracellular fluids, respectively. R, T and F have their usual meanings. E_{rev} was determined by switching to current clamp mode after 5 min of whole-cell recording, a period of sufficient length to allow current activation and also long enough to ensure complete dialysis of the cell by the electrode solution (Pusch & Neher, 1988). The potential recorded in current clamp was subsequently stable (±1 mV) for at least 1 min before it was accepted as a measure of E_{rev}. To further estimate relative anion permeability, the slope conductance (G; calculated as the slope between −100 and −120 mV) was determined in the presence of each anion after 5 min of whole-cell recording.

Since bicarbonate is also thought to pass through an anion channel in choroid plexus (Saito & Wright, 1984), experiments were also performed to estimate P_{HCO_3}/P_{Cl}. In this series the pipette solution contained: 60 mM $NaHCO_3$, 12 mM NaCl, 3 mM $MgCl_2$, 5 mM Na_2ATP, 5 mM BAPTA, 10 mM glucose, 10 mM Hepes, 100 mM mannitol, 0·25 mM cAMP and 375 nM PKA. The pH of the pipette solution was adjusted to 7·2 by addition of 10 M NaOH and the solution was then continuously bubbled with 20% CO_2–80% O_2 prior to use. The corresponding bath solution contained (mM): 18 $NaHCO_3$, 60 NaCl, 1 $CaCl_2$, 1 $MgCl_2$, 10 Hepes, 10 glucose, 120 mannitol. The pH of the bath solution was adjusted to 7·3 by addition of 10 M NaOH and the solution was continuously bubbled with 5% CO_2–95% O_2. For estimation of P_{HCO_3}/P_{Cl}, the bicarbonate concentration was measured before each recording using a Corning 965 CO_2 analyser (Ciba Corning, Essex, UK).

The effect of several anion channel inhibitors on the inwardly rectifying current was also investigated on cells stimulated by cAMP and PKA. The agents used included: the sulphonylurea glibenclamide (Glib; Research Biochemicals International), the stilbene derivative disulphonic 4,4′-diisothiocyanostilbene-2,2′-disulphonic acid (DIDS; Sigma), the arylaminobenzoate 5-nitro-2-(3-phenylpropylamino)-benzoate (NPPB; gift from R. Greger, Freiburg, Germany) and barium (Sigma). Stock solutions (100 mM) of each organic compound were prepared in dimethyl sulphoxide (DMSO; Sigma). These were subsequently diluted in the control bath solution for use in experiments. In separate groups of experiments glibenclamide and NPPB were applied at a concentration of 100 μM. In a further series, DIDS was added at concentrations of both 100 and 500 μM. $BaCl_2$ was added directly to the control bath solution to give a final $[Ba^{2+}]$ of 1 mM.

RNA *in situ* hybridization

RNA *in situ* hybridization was carried out on Wistar rats. Animals were given an overdose of sodium pentobarbitone and tissues were fixed by whole-body perfusion with 4% paraformaldehyde. *In situ* hybridization was carried out essentially as described previously (Trezise *et al.* 1993). Cryostat sections (10 μm) were treated with proteinase K and then hybridized overnight to ^{35}S-labelled single-stranded RNA probes. Two overlapping rat CFTR cDNA clones

were used to synthesize the ^{35}S-labelled riboprobes. These cDNA clones have been described previously and have been used to demonstrate cell-specific expression of CFTR in rat intestine, lung, pancreas, salivary gland and reproductive tracts (Trezise & Buchwald, 1991; Trezise *et al.* 1993). Following hybridization, sections were treated with RNaseA to digest non-hybridized RNA probe and any other single-stranded RNA. Sections were then washed at a stringency of 0·1 × saline sodium citrate (SSC; 15 mM NaCl, 1·5 mM sodium citrate, pH 7·0) at 60 °C. Slides were dipped in Kodak NTB-2 emulsion, left to expose for 2 weeks at 4 °C, developed and counterstained with Haematoxylin and Eosin. Sections were photographed under brightfield and darkfield illumination using a Nikon Optiphot-2 microscope equipped with a Nikon UFX-DX automatic camera. Consecutive sections were hybridized with either an antisense RNA probe to detect CFTR mRNA or with the corresponding sense RNA probe to identify non-specific signals. Where hybridization occurs, the ^{35}S-labelled probe exposes the surrounding photographic emulsion, appearing as white grains under darkfield illumination.

Data presentation and statistics

Unless otherwise stated, data are means ± S.E.M. of observations from n cells. I–V relationships are for the maximum current measured at each applied potential. The extent of current inhibition following drug addition was measured during voltage steps to −120 mV and is expressed as a ratio relative to currents measured immediately before drug addition. Before statistical comparison, ratios were normalized by logarithmic transformation (Zar, 1984). The degree of inhibition was then compared with vehicle controls by one-way analysis of variance (ANOVA) followed by Dunnett's *post hoc* test (Zar, 1984). For determination of the relative anion permeability sequence, values of P_X/P_{Cl} were also log-transformed, then compared for I^- and Br^- using Student's unpaired t test. Student's one-sample t tests were performed to determine whether P_X/P_{Cl} ratios differed from unity. The 5% significance level was adopted throughout.

RESULTS

Cell capacitance and access resistance

The access resistance for all recordings ranged from 6–16 MΩ with a mean of 12·0 ± 0·6 MΩ ($n = 52$). The cell capacitance ranged from 30 to 72 pF, with a mean of 53·8 ± 2·2 pF ($n = 52$). These values are not significantly different from those reported previously for rat choroid plexus (Kotera & Brown, 1994*a*, *b*).

Activation of the inwardly rectifying whole-cell Cl^- current

Figure 1*A* shows a typical control current profile obtained in the absence of cAMP and PKA and using isotonic solutions. In this and four similar recordings small inwardly rectifying currents were observed immediately after the start of whole-cell recording. These currents were sustained, but did not activate further. Figure 1*B* illustrates the marked activation of the inward rectifier resulting from inclusion of cAMP and PKA in the electrode solution. The maximum inward current recorded at −120 mV in the presence of cAMP and PKA (754 ± 83 pA; $n = 21$) was significantly greater (Student's unpaired t test, $P < 0·05$) than in control recordings (317 ± 42 pA; $n = 5$). Current activation was gradual, usually continuing for around 5 min before a stable current level was reached. Such activation was observed in twenty-one out of twenty-three experiments and, once activated, no current run-down was observed in up to 1 h of whole-cell recording.

Use of solutions with a lower $[Cl^-]$ in the pipette (26 mM) than in the bath (144 mM) favours generation of outward rather than inward current (i.e. Goldman rectification). Despite this, only small outward currents were observed. There was no significant difference between maximum outward current measured at +60 mV in the presence of cAMP and PKA (106 ± 13 pA; $n = 21$) compared with control recordings (131 ± 21 pA; $n = 5$). This suggested that the small outward currents observed were not activated by cAMP, but were either leak current or were carried by another conductance. In contrast to the outwardly rectifying currents expected for CFTR when using a low pipette $[Cl^-]$ (Overholt, Saulino, Drumm & Harvey, 1995), inspection of Fig. 1*B* shows the activated current in choroid plexus to be a strong *inward* rectifier. Figure 1*B* also illustrates the presence of time-dependent activation at potentials more hyperpolarized than −80 mV when voltage pulses of 1 s duration were applied. The mean reversal potential for the activated current was −30·9 ± 3·2 mV ($n = 21$), suggesting that it was indeed Cl^- selective ($E_{Cl} = -44$ mV, $E_{Na} = 0$ mV). If it is assumed that Cl^- and aspartate are the only permeant ions (see Methods), then eqn (1) gives a value for $P_{aspartate}/P_{Cl}$ of 0·19 ± 0·05 ($n = 21$).

The I–V relationship for the activated current in Fig. 1*B* resembled that of the voltage-gated channel CLC-2 (Thiemann, Gründer, Pusch & Jentsch, 1992). Since CLC-2 is activated in response to cell swelling, some experiments were performed in which 30 mM mannitol was added to the electrode solution to swell the cells. The use of a hypertonic pipette solution caused the cells to swell gradually (visual inspection under light microscopy) within 5 min of the start of whole-cell recording. Cell swelling was associated with an initial increase in the size of inwardly rectifying currents, but these currents subsequently ran down again within 15 min. At the same time, another current was activated, illustrated in Fig. 1*C*, which was not subject to current run-down thereafter. This outwardly rectifying current was seen in each of five recordings and is similar to volume-activated Cl^- currents reported in many cell types (Kubo &

Okada, 1992). Since this current was not the subject of the present study, its properties are not described here.

Anion selectivity properties of the inward rectifier

Figure 2 illustrates the effect of replacing intracellular Cl^- with either I^- or Br^- as the predominant anion. Comparison of whole-cell currents 5 min after the start of whole-cell recording shows a significantly greater slope conductance in the presence of I^- than Br^-, measured under identical recording conditions (Student's t test, $P < 0{\cdot}05$; Table 1). This suggested that I^- was more permeant than Br^-. Inspection of the reversal potentials showed that currents reversed closer to E_I than to E_{Cl} and use of eqn (1) (see Methods) revealed a value of P_I/P_{Cl} that was significantly greater than unity (Student's one-sample t test, $P < 0{\cdot}05$; Table 1). By contrast, in the presence of Br^- the reversal potential was closer to E_{Cl} than E_{Br} and P_{Br}/P_{Cl} was significantly less than unity (Student's one-sample t test, $P < 0{\cdot}05$; Table 1). Taken together these experiments suggest a halide selectivity sequence of $I^- > Cl^- > Br^-$.

In an additional series of experiments P_{HCO_3}/P_{Cl} was estimated using 60 mM $NaHCO_3$ in the pipette solution (Fig. 2*C*). Under these conditions, the process of activation of the inward rectifier was less stable than that seen previously and there was greater variation in the size of currents observed. Nevertheless, these data provide an estimate of P_{HCO_3}/P_{Cl} of $1{\cdot}5 \pm 0{\cdot}5$, which is not significantly different from unity, but was significantly greater than zero (Student's one-sample t test, $P < 0{\cdot}05$), suggesting that HCO_3^- is able to permeate the cAMP-regulated anion channel.

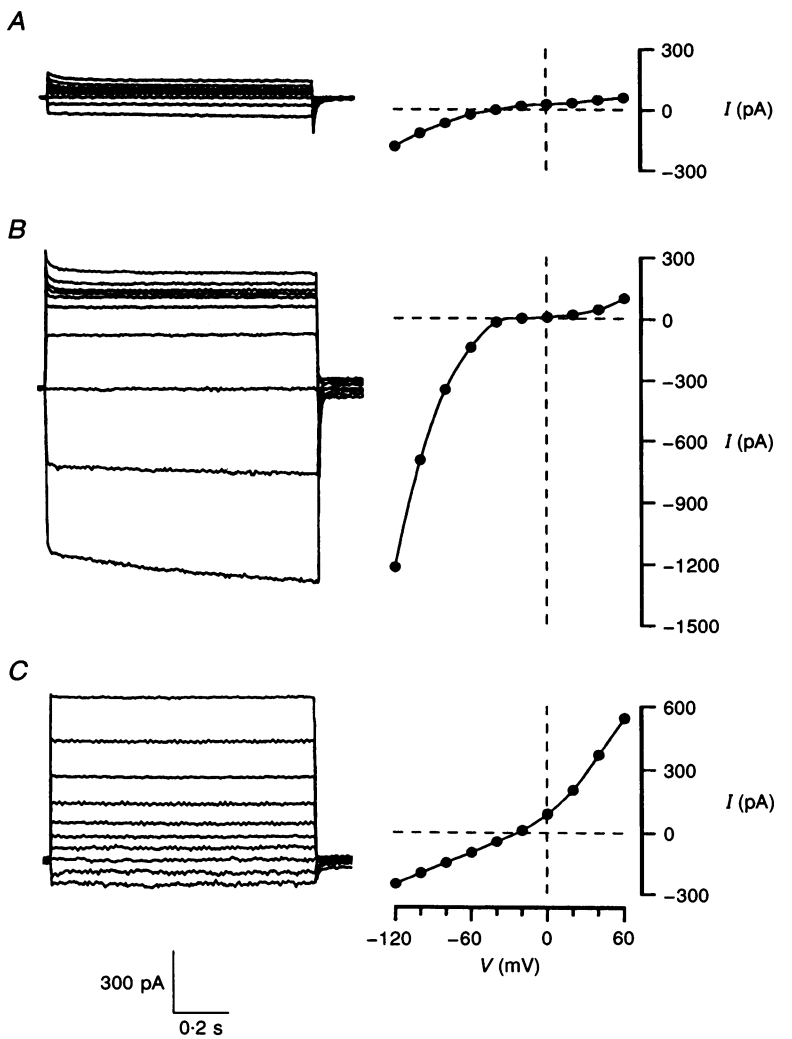

Figure 1. Stimulation of cAMP-dependent and volume-activated whole-cell currents

The panels on the left show representative current profiles obtained by applying 1 s voltage steps from −120 to +60 mV in increments of 20 mV; voltage steps were applied from a holding potential of −80 mV and were separated by a 3 s delay. The I–V relationships for each respective current profile are illustrated on the right. *A*, currents obtained using control solutions in the absence of cAMP and PKA; *B*, activation of inwardly rectifying current by addition of cAMP and PKA to the control electrode solution; *C*, activation of outwardly rectifying, swelling-activated currents using a 30 mosmol kg^{-1} hypertonic pipette solution.

Table 1. Relative anion permeabilities

Anion (X^-)	n	E_{rev} (mV)	P_X/P_{Cl}	G_X (nS)
I^-	5	+21·6 ± 4·3	3·5 ± 0·8*	18·0 ± 4·0*
Br^-	6	−9·2 ± 1·9	0·6 ± 0·1	7·0 ± 2·1
HCO_3^-	5	−1·6 ± 3·9	1·5 ± 0·5	5·5 ± 1·1
Aspartate	21	−30·9 ± 3·2	0·2 ± 0·1	11·7 ± 1·5

Data are means ± S.E.M. Current reversal potentials (E_{rev}) were measured at least 5 min after achieving the whole-cell recording configuration and values were stable in the range ±1 mV. P_X/P_{Cl} was calculated from the Goldman–Hodgkin–Katz equation (eqn (1); see Methods). The slope conductance (G) was measured between −100 and −120 mV after 5 min of whole-cell recording. * Significant differences between values of P_X/P_{Cl} and G for I^- and Br^- (Student's t test, $P < 0·05$).

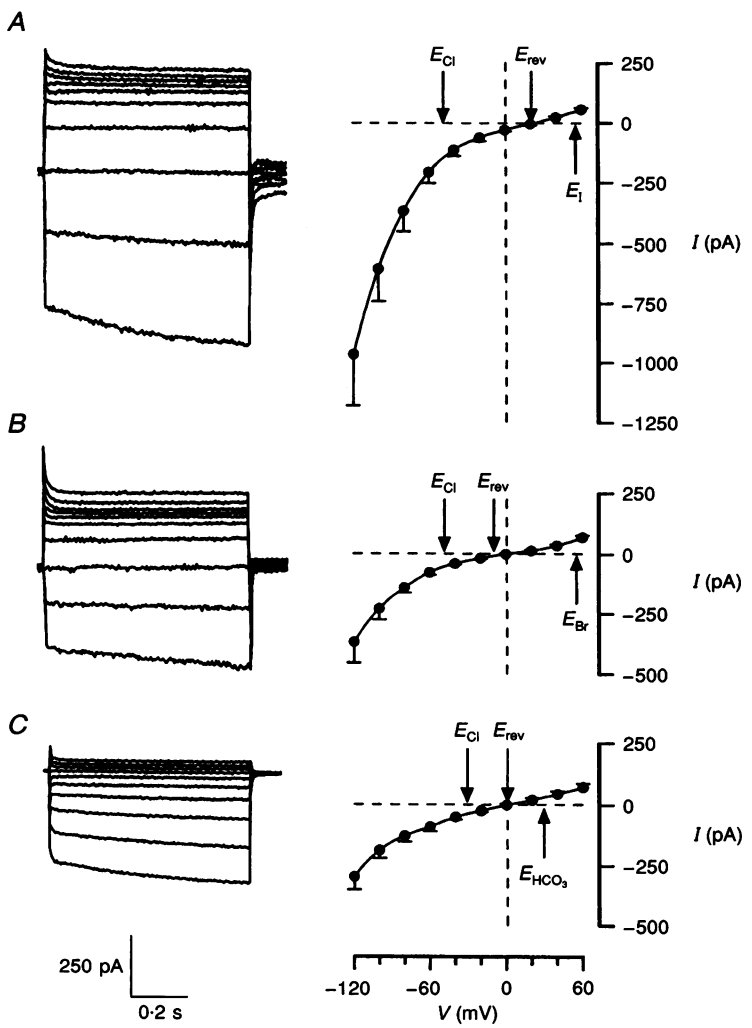

Figure 2. Anion selectivity of the cAMP-dependent whole-cell current

A, permeation by I^-; *B*, permeation by Br^-. The concentrations of replacement halide in the pipette and bath solutions were 110 and 12 mM, respectively. *C*, permeation by HCO_3^-. The HCO_3^- concentrations in the pipette and bath solutions were 60 and 18 mM, respectively. In all cases, currents were activated by addition of cAMP and PKA to the electrode solution. Representative current profiles obtained with each replacement anion, using the voltage protocol described in Fig. 1, are shown on the left. *I–V* relationships were obtained 5 min after the start of whole-cell recording and are shown on the right; data are means ± S.E.M. (I^-, $n = 5$; Br^-, $n = 6$; HCO_3^-, $n = 5$). E_{rev}, reversal potential; E_X, equilibrium potential.

Effect of various channel inhibitors on inwardly rectifying Cl^- currents

The first compound tested was the sulphonylurea glibenclamide, since this is a known blocker of CFTR Cl^- currents (Sheppard & Welsh, 1992). The addition of 100 μM glibenclamide to the bath solution caused inhibition of the inward rectifier. This is illustrated in Fig. 3, where it can be seen that currents recorded during voltage pulses to −120 mV were substantially reduced (Fig. 3*A*). Current inhibition was incomplete, however, since the residual current still displayed inward rectification rather than the linear currents expected for a background leak current (Fig. 3*B*). The time course of glibenclamide inhibition is shown in Fig. 3*C*, where it can be seen that the decline in inward current began during the first minute of glibenclamide addition and continued towards a current minimum during the next 5 min. The mean inhibition of currents measured during 1 s voltage steps to −120 mV was 48·3 ± 7·9% ($n = 5$; see also Fig. 5). Inhibition by glibenclamide was only fully reversible in one out of five recordings. This could not be explained by a fall in the access conductance, however, which was constant throughout each recording. The observation that cAMP does not significantly increase outward currents (see above) suggested that CFTR Cl^- currents are undetectable in choroid plexus. Figure 3 also shows that the small outward currents which were observed could not be blocked by glibenclamide. Since this sulphonylurea is a known blocker

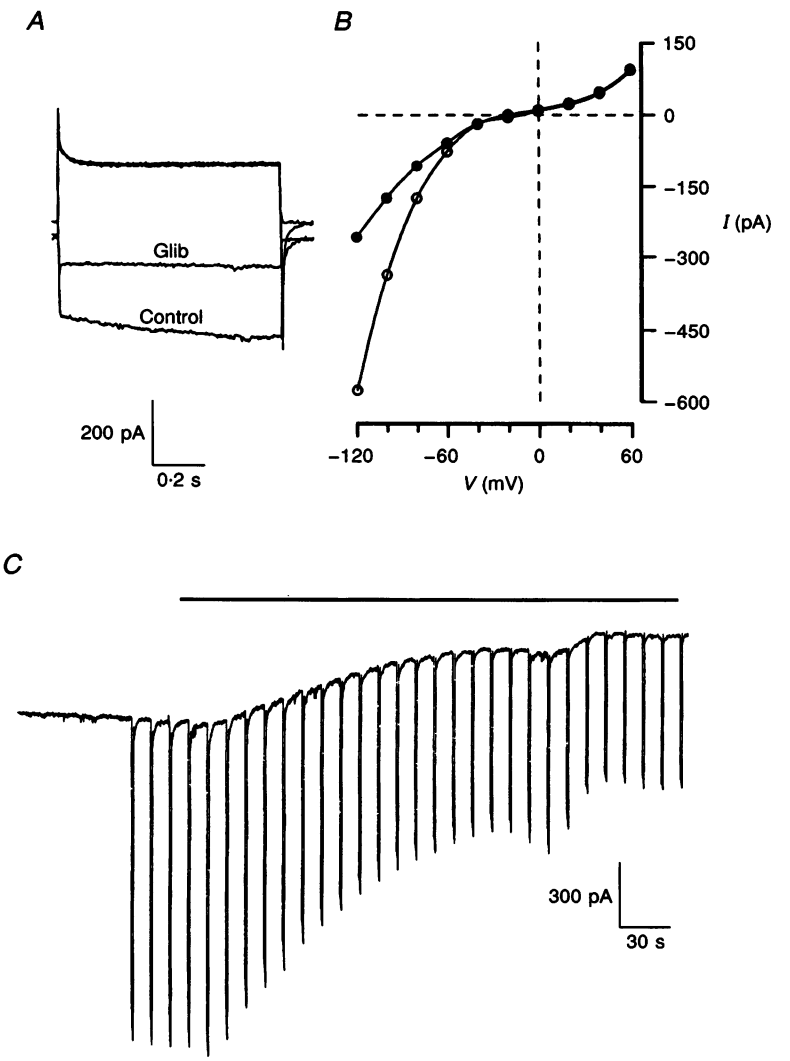

Figure 3. Glibenclamide blocks inwardly rectifying whole-cell Cl^- currents

A, superimposed currents recorded from 1 s voltage steps to −120 and +60 mV before and after addition of 100 μM glibenclamide (Glib). *B*, complete *I–V* relationships for currents shown in *A* (○, control; ●, 100 μM glibenclamide). *C*, representative example of the time course of glibenclamide-induced current inhibition obtained by applying 1 s voltage pulses to −120 mV from a holding potential of −80 mV at a frequency of 0·1 Hz; the horizontal bar indicates the period of glibenclamide addition.

of CFTR (Sheppard & Welsh, 1992), these data strongly suggest that CFTR Cl^- currents are not present in the rat choroid plexus.

The inwardly rectifying Cl^- current was also sensitive to inhibition by the stilbene derivative DIDS at concentrations of both 100 and 500 μM. The effect of 500 μM DIDS on inward currents (Fig. 4*A*) was similar to the partial inhibition seen with glibenclamide. Addition of 100 μM DIDS caused 27·4 ± 7·7% ($n = 7$) reduction of currents measured at −120 mV and the subsequent addition of 500 μM DIDS increased the degree of this inhibition to 50·5 ± 6·1% ($n = 5$; Figs 4*A* and 5). In contrast to glibenclamide, DIDS caused a slight reduction in the outward current (Fig. 4*A*). This may reflect voltage dependence of inhibition by DIDS, with a greater effect at depolarizing voltages than glibenclamide. In each case the inhibition by DIDS was only partly reversible. Application of the arylaminobenzoate NPPB at a dose of 100 μM also resulted in partial block of the cAMP-dependent Cl^- current (Fig. 4*B*). Blockade by NPPB was rapid in onset and was also largely reversible. The mean inhibition of currents recorded at −120 mV following 100 μM NPPB application was 30·8 ± 4·1% ($n = 6$; Fig. 5).

Figure 5 summarizes the extent of inhibition of the cAMP-activated inwardly rectifying Cl^- current by each of the anion channel inhibitors applied. Inhibition was measured during 1 s voltage pulses to −120 mV. Addition of 0·1% DMSO vehicle had no significant effect on the activated Cl^- current. When compared with this vehicle control, each substance tested produced a significant degree of current inhibition (ANOVA plus Dunnett's, $P < 0·05$).

Glibenclamide, DIDS and NPPB are all well-known blockers of Cl^- channels. Recent experiments have also shown that Ba^{2+} inhibits inwardly rectifying Cl^- currents associated with the protein phospholemman (Moorman, Palmer, John, Durieux & Jones, 1992). In three experiments, Ba^{2+} caused a substantial inhibition of the inward rectifier (Fig. 6), which was entirely reversible in each case. The mean inhibition following addition of 1 mM Ba^{2+} was 73·0 ± 5·3% ($n = 3$). These experiments were performed using I^- as the main current carrier (see Fig. 2).

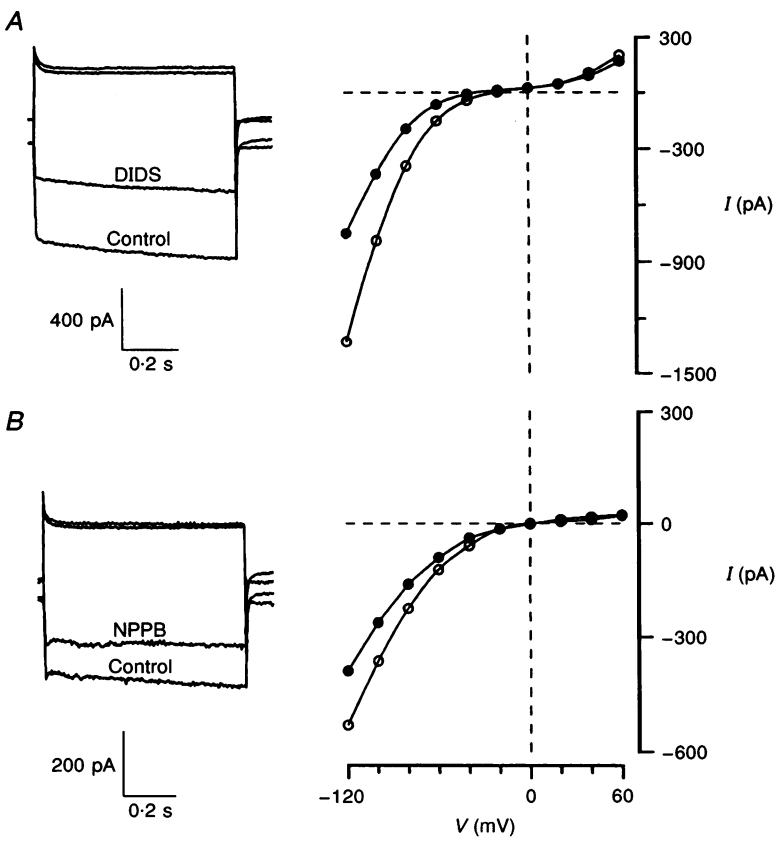

Figure 4. Inhibition of inwardly rectifying whole-cell Cl^- currents by DIDS and NPPB

A, effect of 500 μM DIDS; *B*, effect of 100 μM NPPB. The panels on the left show superimposed currents recorded from 1 s voltage steps to −120 and +60 mV before and after addition of drug. The panels on the right show complete *I–V* relationships for currents shown on the left (○, control; ●, drug).

In situ hybridization

The electrophysiological characterization of the cAMP-dependent Cl^- current present in the choroid plexus suggested that the channel protein underlying the current was unlikely to be CFTR (see Discussion). RNA *in situ* hybridization experiments were therefore performed to see whether CFTR expression could be detected in this tissue. The results are presented in Fig. 7 which shows brightfield and darkfield views of choroid plexus hybridized with antisense (Fig. 7*A* and *B*) and sense (Fig. 7*C* and *D*) rat CFTR cRNA probes. No signal could be detected above background in any region of the choroid plexus. These data were obtained using two rats in separate hybridization experiments. A minimum of eight sections were taken in each experiment and two independent cRNA probes were used in each case. Using the same fixation and hybridization conditions, CFTR mRNA has been detected in pancreatic and salivary gland ducts, intestine, bronchi and bronchioles, and testis (Trezise & Buchwald, 1991; Trezise *et al.* 1993).

DISCUSSION

This study investigated the pharmacology and halide selectivity properties of the cAMP-activated Cl^- current in choroid plexus epithelial cells in order to compare it with current associated with known Cl^- channels, particularly CFTR.

Comparison of the properties of the inward rectifier with CFTR

In patch clamp experiments several lines of evidence suggested that the cAMP-activated Cl^- current in choroid plexus was not carried by CFTR. First, despite using conditions which favoured their generation, outward Cl^- currents were small and, furthermore, the activated current showed pronounced inward rectification. Second, the halide selectivity sequence for the activated current was $I^- > Cl^- > Br^-$, which is quite distinct from the sequence $Br^- > Cl^- > I^-$ for CFTR (Anderson *et al.* 1991). Third, the activated inwardly rectifying current was sensitive to inhibition by the stilbene derivative DIDS which does not affect CFTR (Kartner *et al.* 1991). Finally, those small outward currents which were observed in the presence of cAMP and PKA were not inhibited by glibenclamide, which is a known blocker of CFTR (Sheppard & Welsh, 1992), Thus, we found no evidence of CFTR-mediated Cl^- currents in cells from the rat choroid plexus.

In support of these functional data our RNA *in situ* hybridization experiments failed to detect any signal for CFTR. The protocol used for RNA *in situ* hybridization can reliably detect CFTR mRNA in adult rat lung (Trezise & Buchwald, 1991). The level of CFTR mRNA in rat lung is similar to that in human lung (Engelhardt *et al.* 1992), where it has been estimated that one to two copies of mRNA are expressed per cell (Trapnell *et al.* 1991). Since

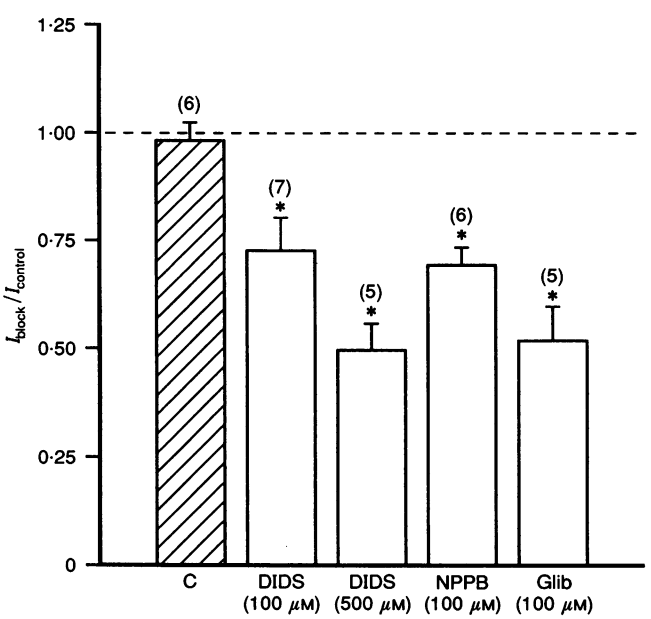

Figure 5. Mean inhibition of inwardly rectifying whole-cell Cl^- currents by glibenclamide, DIDS and NPPB

Data are means ± S.E.M. for the ratio of current measured during voltage steps to −120 mV before and after drug addition. The hatched bar indicates the effect of 0·1% DMSO vehicle. The number of cells in each group is indicated in parentheses. The agent and concentration applied are indicated on the *x*-axis. * Significant inhibition by a drug relative to vehicle control (C) (ANOVA plus Dunnett's, $P < 0·05$).

CFTR expression was not detected in the rat choroid plexus, this suggests that CFTR is either not expressed in this tissue, or is expressed at less than two copies of mRNA per cell. Hincke *et al.* (1995) reported that CFTR is expressed in some cells of the rat choroid plexus, using immunocytochemical localization. The reason for this discrepancy is unclear, but could relate to antibodies raised against CFTR cross-reacting with some other protein expressed in the choroid plexus.

At present, we cannot rule out the possibility that the choroid plexus has a very low level of CFTR expression, which may have a function other than as a cAMP-regulated Cl^- channel, e.g. CFTR is thought to play a role as a regulator of other ion channels (Schweibert *et al.* 1995; Stutts *et al.* 1995). Such a role in the choroid plexus is difficult to assess at present, since this will require experiments using knockout mice that lack the CFTR gene product (Colledge, Ratcliff, Foster, Williamson & Evans, 1992). In conclusion, properties of the inward rectifier indicate that it is distinct from CFTR and, furthermore, that CFTR-mediated Cl^- currents are not detectable in rat choroid plexus epithelial cells.

Comparison with other Cl^- channels

Although the molecular identity of the choroid plexus channel is at present unresolved, the channel does share properties with other types of Cl^- channel. One obvious comparison is with CLC-2, an inwardly rectifying member of the CLC voltage-gated channel family, which is activated by cell swelling (Thiemann *et al.* 1992). The expression of this channel in choroid plexus has not yet been investigated and although the inward rectifier in the choroid plexus transiently increased in size during cell swelling, other properties of this channel differ from CLC-2. When CLC-2 is expressed in *Xenopus* oocytes it displays an anion selectivity sequence $Cl^- > Br^- > I^-$, and the predicted nucleotide sequence lacks consensus sites for PKA

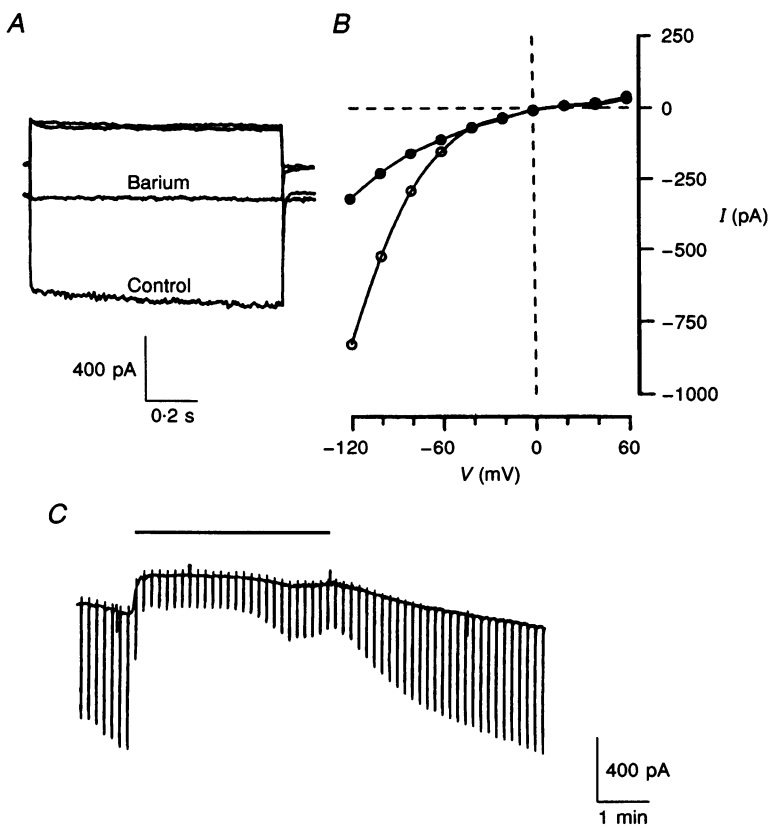

Figure 6. Effect of Ba^{2+} on inwardly rectifying whole-cell Cl^- currents

A, superimposed currents recorded from voltage steps to −120 and +60 mV before and after addition of 1 mM Ba^{2+}. *B*, complete *I–V* relationships for currents shown in *A* (○, control; ●, 1 mM Ba^{2+}). *C*, representative example of the time course of Ba^{2+}-induced current inhibition obtained by applying 1 s voltage pulses to −120 mV from a holding potential of −80 mV at a frequency of 0·1 Hz; the horizontal bar indicates the period of Ba^{2+} addition. Experiments with Ba^{2+} were performed using I^- as the main current carrier (see Fig. 2).

phosphorylation (Thiemann *et al.* 1992), which are presumably required to explain the activation by cAMP and PKA we describe in choroid plexus. Thus, the inward rectifier in choroid plexus is unlikely to be CLC-2. It should be pointed out that CLC-2G, a channel from the rabbit gastric parietal cell, which is closely related to CLC-2, does have consensus sites for PKA-mediated phosphorylation (Malinowska, Kupert, Bahinski, Sherry & Cuppoletti, 1995). In common with the current we describe in the present study, single channel recordings of CLC-2G show the relative halide permeability to be $I^- > Cl^-$ (Malinowska *et al.* 1995). However, single channel records also showed that current carried by CLC-2G was linear rather than inwardly rectifying. It is also interesting to note that cells from *Necturus* gastric mucosa express a cAMP-activated Cl^- channel which does show inward rectification in cell-attached patches (Demarest, Loo & Sachs, 1989). This channel is not, however, likely to be the same as the one we describe in choroid plexus, because it was insensitive to external Ba^{2+}.

The current described in the choroid plexus also shows similarities to the current associated with phospholemman, a peptide which induces time-dependent inwardly rectifying currents when overexpressed in *Xenopus* oocytes (Moorman *et al.* 1992). Phospholemman is also a known substrate for PKA and is blocked by Ba^{2+} (Moorman *et al.* 1992). Unitary currents of phospholemman were recently recorded in planar lipid bilayers (Moorman *et al.* 1995) and were found to have a very large conductance (700 pS). The halide permeation properties were similar to those reported here ($I^- > Cl^- > Br^-$), but Na^+ was also permeant ($P_{Na}/P_{Cl} = 0{\cdot}3$), which differs from our previous findings for the channel in choroid plexus (Kotera & Brown, 1994*a*). To our knowledge there is no information at present regarding the expression of phospholemman at the molecular level in choroid plexus and this will clearly be an important approach in future to determine the identity of the cAMP-activated Cl^- channel in choroid plexus.

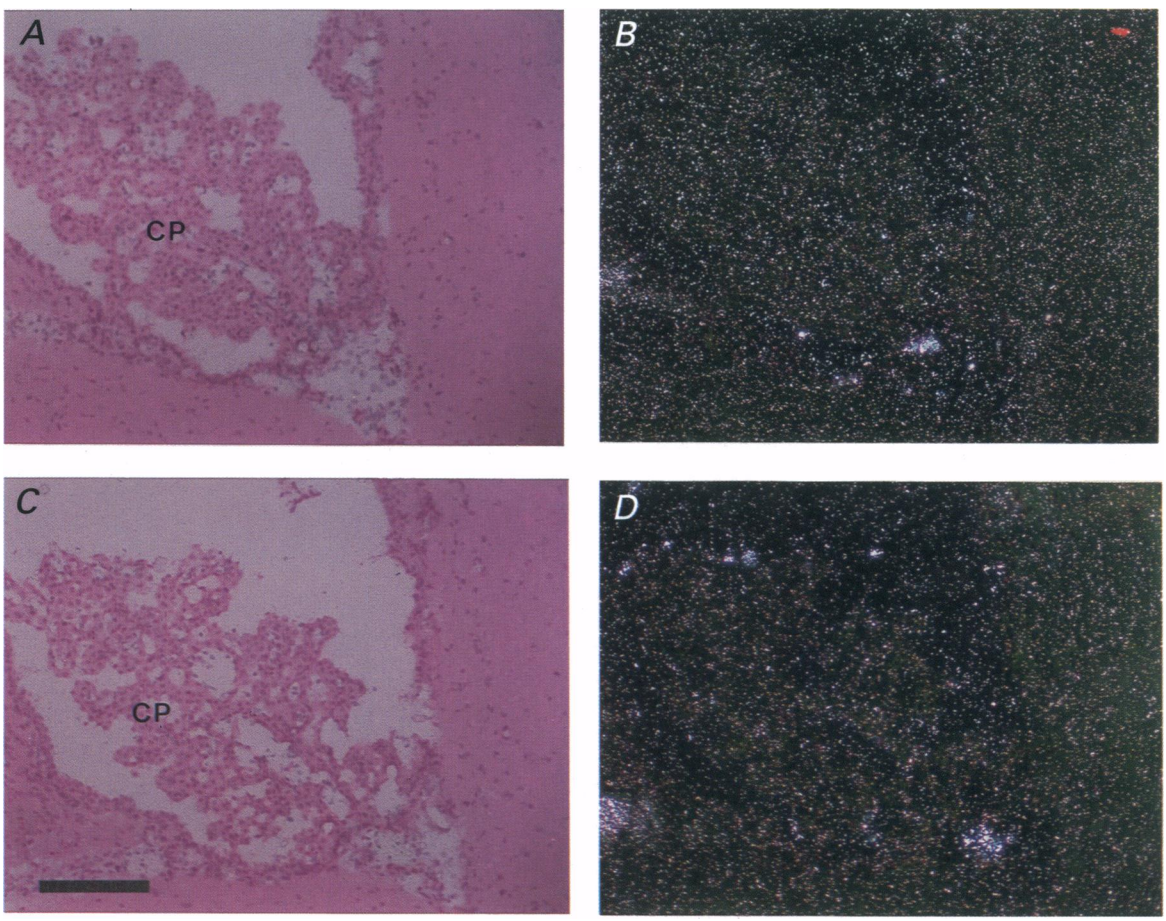

Figure 7. RNA *in situ* hybridization for CFTR in rat choroid plexus

A and *B*, brightfield and darkfield views, respectively, of a section of rat brain hybridized with an antisense strand, rat CFTR cRNA probe. *C* and *D*, brightfield and darkfield views, respectively, of a consecutive section of rat brain hybridized with a sense strand rat CFTR cRNA probe. CP denotes choroid plexus. The scale bar is equivalent to 200 μm.

Possible physiological role of the inward rectifier

Several studies have described an increase in CSF production stimulated by cAMP (e.g. Epstein, Feldman & Brusilow, 1977). This increase in CSF secretion is driven by activation of a conductive pathway in the apical cell membrane, which mediates both Cl^- and HCO_3^- efflux (Saito & Wright, 1983; Deng & Johanson, 1992). Several properties of the channel described in the present study suggest that it may be responsible for the increase in CSF production stimulated by cAMP. First, as an inward rectifier it preferentially mediates Cl^- secretion from the cell. Second, this channel is open at physiological membrane potentials (−20 to −80 mV). Third, the inward rectifier in choroid plexus is open at normal cell volume and can be observed from the start of whole-cell experiments, even in the absence of cAMP stimulation. Fourth, the present study shows that bicarbonate can pass through the inward rectifier. Finally, this channel appears to be conserved among species, being present in rat, mouse (J. D. Kibble, unpublished observations) and also *Necturus* (Birnir, Loo, Brown & Wright, 1989). The cAMP-activated anion current characterized in the present study is likely to be the same as that observed by others using short-circuit current measurements (Saito & Wright, 1983), intracellular microelectrode recordings (Saito & Wright, 1984) and Cl^- flux studies (Deng & Johanson, 1992).

In conclusion, the anion selectivity properties, pharmacology and kinetics of the cAMP-activated Cl^- current present in rat choroid plexus differ markedly from those of CFTR. In addition, we could not detect CFTR mRNA in rat choroid plexus by RNA *in situ* hybridization, consistent with the view that CFTR does not contribute to cAMP-dependent Cl^- currents in this tissue. Properties of the inward rectifier had some similarity with, but were not identical to, currents associated with other voltage-gated Cl^- channels such as CLC-2 and phospholemman.

Anderson, M. P., Gregory, R. J., Thompson, S., Souza, D. W., Paul, S., Mulligan, R. C., Smith, A. E. & Welsh, M. J. (1991). Demonstration that CFTR is a chloride channel by alteration of its anion selectivity. *Science* **253**, 202–205.

Birnir, B., Loo, D. D. F., Brown, P. D. & Wright, E. M. (1989). Whole-cell currents in *Necturus* choroid plexus. *FASEB Journal* **2**, A1722.

Colledge, W. H., Ratcliff, R., Foster, D., Williamson, R. & Evans, M. J. (1992). Cystic fibrosis mouse with intestinal obstruction. *Lancet* **340**, 680.

Demarest, J. R., Loo, D. D. F. & Sachs, G. (1989). Activation of apical Cl^- channels in the gastric oxyntic cell. *Science* **245**, 402–404.

Deng, Q.-S. & Johanson, C. E. (1992). Cyclic AMP alteration of chloride transport into the choroid plexus–cerebrospinal fluid system. *Neuroscience Letters* **143**, 146–150.

Engelhardt, J. F., Yankaskas, J. R., Ernst, S. A., Yang, Y., Marino, C. R., Boucher, R. C., Cohn, J. A. & Wilson, J. M. (1992). Submucosal glands are the predominant site of CFTR expression in the human bronchus. *Nature Genetics* **2**, 240–248.

Epstein, M. H., Feldman, A. M. & Brusilow, S. W. (1977). Cerebrospinal fluid production: stimulation by cholera toxin. *Science* **196**, 1012–1013.

Fuller, C. M. & Benos, D. J. (1992). CFTR! *American Journal of Physiology* **263**, C267–286.

Hamill, O. P., Marty, A., Neher, E., Sakmann, B. & Sigworth, F. J. (1981). Improved patch-clamp techniques for high-resolution current recording from cells and cell-free membrane patches. *Pflügers Archiv* **391**, 85–100.

Hincke, M. T., Nairn, A. C. & Staines, W. A. (1995). Cystic fibrosis transmembrane conductance regulator is found within brain ventricular epithelium and choroid plexus. *Journal of Neurochemistry* **64**, 1662–1668.

Kartner, N., Hanrahan, J. W., Jensen, T. J., Naismith, A. L., Sun, S., Ackerly, A., Reyes, E. F., Tsui, L.-C., Rommens, J. M., Bear, C. E. & Riordan, J. R. (1991). Expression of the cystic fibrosis gene in non-epithelial invertebrate cells produces a regulated anion conductance. *Cell* **64**, 681–691.

Kotera, T. & Brown, P. D. (1994*a*). Cl^- current activation in choroid plexus epithelial cells involves a G-protein and protein kinase A. *American Journal of Physiology* **266**, C536–540.

Kotera, T. & Brown, P. D. (1994*b*). Evidence for two types of potassium current in rat choroid plexus epithelial cells. *Pflügers Archiv* **427**, 317–324.

Kubo, M. & Okada, Y. (1992). Volume-regulatory Cl^- currents in cultured human epithelial cells. *Journal of Physiology* **456**, 351–371.

Malinowska, D. H., Kupert, E. Y., Bahinski, A., Sherry, A. M. & Cuppoletti, J. (1995). Cloning, functional expression, and characterization of a PKA-activated gastric Cl^- channel. *American Journal of Physiology* **268**, C191–200.

Moorman, J. R., Ackerman, S. J., Kowdley, G. C., Griffin, M. P., Mounsey, J. P., Chen, Z., Cala, S. E., O'Brian, J. J., Szabo, G. & Jones, L. R. (1995). Unitary anion currents through phospholemman channel molecules. *Nature* **377**, 737–740.

Moorman, J. R., Palmer, C. J., John, J. E. III, Durieux, M. E. & Jones, L. R. (1992). Phospholemman expression induces a hyperpolarization-activated chloride current in *Xenopus* oocytes. *Journal of Biological Chemistry* **267**, 14551–14554.

Overholt, J. L., Saulino, A., Drumm, M. L. & Harvey, R. D. (1995). Rectification of whole-cell cystic fibrosis transmembrane conductance regulator current. *American Journal of Physiology* **268**, C636–646.

Pusch, M. & Neher, E. (1988). Rates of diffusional exchange between small cells and a measuring patch pipette. *Pflügers Archiv* **411**, 204–211.

Saito, Y. & Wright, E. M. (1983). Bicarbonate transport across the frog choroid plexus and its control by cyclic nucleotides. *Journal of Physiology* **336**, 635–648.

Saito, Y. & Wright, E. M. (1984). Regulation of bicarbonate transport across the brush border membrane of the bull-frog choroid plexus. *Journal of Physiology* **350**, 327–342.

Schweibert, E. M., Egan, M. E., Hwang, T. H., Fulmer, S. B., Allen, S. S., Cutting, G. R. & Guggino, B. (1995). CFTR regulates outwardly-rectifying chloride currents through an autocrine mechanism involving ATP. *Cell* **81**, 1063–1073.

SEGAL, M. B. (1993). Extracellular and cerebrospinal fluid. *Journal of Inherited Metabolic Disease* **16**, 617–638.

SHEPPARD, D. N. & WELSH, M. J. (1992). Effect of ATP-sensitive K^+ channel regulators on cystic fibrosis transmembrane conductance regulator chloride currents. *Journal of General Physiology* **100**, 573–591.

STUTTS, M. J., CANESSA, C. M., OLSEN, J. C., HAMRICK, M., COHN, J. A., ROSSITER, B. C. & BOUCHER, R. C. (1995). CFTR as a cAMP-dependent regulator of sodium channels. *Science* **269**, 847–850.

THIEMANN, A., GRÜNDER, S., PUSCH, M. & JENTSCH, T. J. (1992). A chloride channel widely expressed in epithelial and non-epithelial cells. *Nature* **356**, 57–60.

TRAPNELL, B. C., CHU, C. S., PAAKKO, P. K., BANKS, T. C., YOSHIMURA, K., FERRANS, V. J., CHERNICK, M. S. & CHYSTAL, R. G. (1991). Expression of the cystic fibrosis transmembrane conductance regulator gene in the respiratory tract of normal individuals and individuals with cystic fibrosis. *Proceedings of the National Academy of Sciences of the USA* **88**, 6565–6569.

TREZISE, A. E. O. & BUCHWALD, M. (1991). *In-vivo* cell-specific expression of the cystic fibrosis transmembrane conductance regulator. *Nature* **353**, 434–437.

TREZISE, A. E. O., LINDER, C. C., GRIEGER, D., THOMPSON, E. W., MEUNIER, H., GRISWOLD, M. D. & BUCHWALD, M. (1993). CFTR expression is regulated during both the cycle of the seminiferous epithelium and the oestrous cycle of rodents. *Nature Genetics* **3**, 157–164.

ZAR, J. H. (1984). *Biostatistical Analysis*. Prentice Hall International Inc., New Jersey.

Acknowledgements

This work was supported by The Wellcome Trust (grant 037321/2/92), the Medical Research Council and the Imperial Cancer Research Fund.

Author's email address

J. D. Kibble: j.kibble@man.ac.uk

Received 16 April 1996; accepted 10 June 1996.